中国激光

平行平面腔光学参量振荡器失谐特性实验研究

付俏俏[1,2,5]，刘鹏翔[1,2,4*]，祁峰[1,2,4]，李惟帆[1,2,4]，牛春草[1,2,3]，李伟[1,2,3]，郭丽媛[1,2]，汪业龙[1,2,4]，刘朝阳[1,2,4]

[1]中国科学院沈阳自动化研究所，辽宁 沈阳 110169；

[2]辽宁省太赫兹成像与感知重点实验室，辽宁 沈阳 110169；

[3]沈阳化工大学信息工程学院，辽宁 沈阳 110142；

[4]中国科学院机器人与智能制造创新研究院，辽宁 沈阳 110169；

[5]中国科学院大学，北京 100049

摘要 纳秒脉冲泵浦的平行平面腔光学参量振荡器(OPO)是一种便捷的相干光源，适用于指定波长范围内的不间断调谐输出。作为一种临界腔，平行平面腔对腔镜准直角度的扰动较为敏感。本文以532 nm绿光泵浦$KTiOPO_4$晶体临界相位匹配OPO为例，定量研究了这类光谐振腔的失谐特性。通过在理想准直位置附近扫描腔镜的偏角，观察了OPO输出随失谐角的变化。结果表明：该谐振腔对临界方向失谐的敏感程度远高于对非临界方向失谐的敏感程度；扩宽泵浦光束和提高泵浦光强都可以增大对准容限。此外，本文分析并解释了不同条件下OPO腔长对腔镜对准容限的影响。

关键词 非线性光学；光学参量振荡器；平行平面腔；对准容限；临界相位匹配

中图分类号 O437 **文献标志码** A **DOI**：10.3788/CJL202249.2408002

1 引 言

光学参量振荡器(OPO)极大地扩展了相干光源的输出波长范围，将有限的商用激光波长(通常为固定的发射线或较窄的发射带)扩展为从可见光到远红外波段的不间断覆盖[1]。高峰值功率的调Q激光器进一步推动了OPO的发展，使其具有紧凑的结构(如只需两个腔镜和一个非线性晶体)、较高的转换效率和单谐振运转等优点，成为实现指定波长相干光产生的一种有效手段。平行平面腔是最早提出的激光谐振腔型，在OPO(特别是脉冲运转OPO)中被广泛采用。基于这类光腔的OPO具有大的模体积，易于准直，而且能够实现大范围角度调谐，因此被大量用作非线性太赫兹和中红外光源的泵浦/种子源[2-4]，或直接作为中红外光源[5-7]。

平行平面腔属于临界腔，对腔镜准直角度的扰动(失谐)较为敏感[8]。针对激光器的腔失谐研究主要集中在20世纪60—80年代，实验工作主要涉及氩离子激光器[9]、CO_2激光器[10]和Nd:YAG激光器[11-13]等，计算分析最初建立在微扰理论框架下[11-12]，后来发展出了考虑空间变化的速率方程模型[13]。1979年，原杭州大学王绍民[14]完整地阐述了非共轴(失谐)系统光束传输的矩阵和图论处理方法；1984年，中国科学院上海光学精密机械研究所方洪烈等[15]利用多尺度微扰方法推导了失谐平行平面腔积分方程的解析解；1986年，四川大学吕百达[16]综合分析了失谐腔的几种理论方法，包括几何光学法、高斯光束法、衍射积分方程法和矩阵光学法；2001年，中国科学院西安光学精密机械研究所胡亚红等[17]提出了一种基于光斑边缘检测的谐振腔失谐自动校正方法，并采用He-Ne激光器进行了验证。所查资料鲜有对OPO腔的相关研究。

本团队研究了平行平面腔OPO的失谐特性，搭建了532 nm绿光激光泵浦$KTiOPO_4$(KTP)晶体的OPO装置。该装置代表了纳秒脉冲泵浦临界相位匹配OPO这类结构。本团队观察并解释了腔镜对准容限在不同方向上的显著差异，分析了对准容限随光束尺寸、泵浦强度和腔长等参数的变化。

2 实验装置

KTP晶体平行平面腔OPO(KTP-OPO)的结构如图1所示。倍频Nd:YAG调Q激光器(紫玉激光)作为泵浦源，波长为532 nm，脉冲宽度为10 ns，重复频率为10 Hz。参量晶体KTP的尺寸为10 mm×7 mm×20 mm，极角$\theta=60°$，方位角$\varphi=0°$，通光面镀532 nm、

收稿日期：2022-03-18；**修回日期**：2022-04-12；**录用日期**：2022-05-07

基金项目：中国科学院青年创新促进会资助项目(2019204)、辽宁省“兴辽英才”计划(XLYC200774)、沈阳市中青年科技创新人才项目(RC200512)

通信作者：*liupengxiang@sia.cn

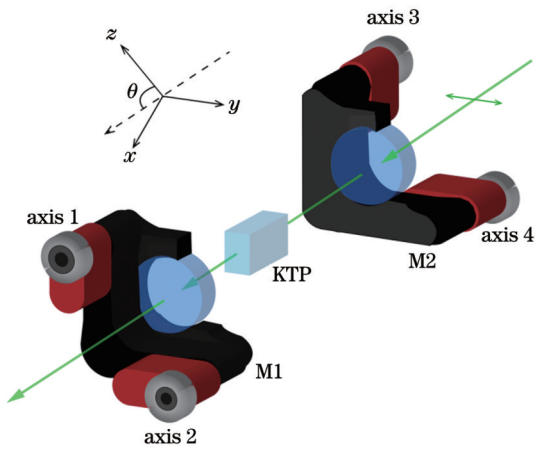

图 1　KTP 晶体平行平面腔 OPO 的结构图

Fig. 1　Structure of plane-parallel cavity based KTP-OPO

800～900 nm 和 1300～1600 nm 增透膜。谐振腔由两块相同的镀膜平面镜 M1 和 M2 组成，M1 和 M2 对 532 nm 泵浦光和 1514 nm 闲频光高透，对 820 nm 信号光高反，形成单谐振。三个波长满足 o → e（信号光）+ o（闲频光）形式的二类临界相位匹配[18]。每个腔镜均通过配备有两个压电促动器的二维光学调整架（newfocus 8816-6）进行控制，通过调整架调整腔镜的准直效果，并保证腔镜能够在理想的准直位置附近沿两个方向（输出镜 M1 的 1 轴、2 轴以及输入镜 M2 的 3 轴、4 轴）进行扫描。二维光学调整架的角度分辨率小于等于 0.7 μrad。

3　实验结果分析与讨论

该 KTP-OPO 的输出结果如图 2 所示。使用硅基和 InGaAs 基光电二极管（Newport 1621 和 Newport 1623）测量输入泵浦光（虚线）、输出闲频光（实线）和剩余泵浦光（点线）的同步脉冲包络。输入和输出脉冲宽度分别为 10.2 ns 和 8.4 ns。图中反映了脉冲 OPO 的运转动态，包括闲频光的增长和泵浦光的消耗，与已有

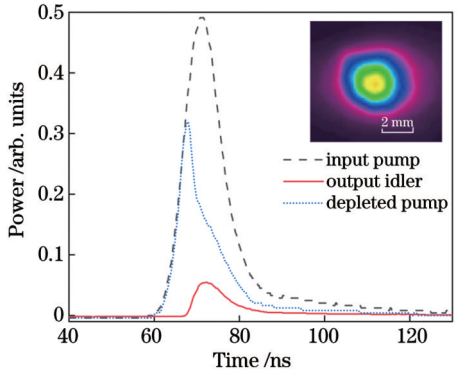

图 2　KTP-OPO 输入泵浦光（虚线）、输出闲频光（实线）和剩余泵浦光（点线）的脉冲包络，插图为 OPO 输出光束的轮廓

Fig. 2　Pulse envelops of KTP-OPO input pump (dashed), output idler (solid) and depleted pump (dotted), where the inset exhibits OPO output beam profile

报道[19-20]相符。插图为热释电相机（Ophir PY-IV）获得的闲频光近场（距 M1 约 40 mm）光束轮廓，使用光谱仪（AQ6370D）测得闲频光波长为 1514 nm。水平和垂直方向的光束直径（峰值 $1/e^2$ 全宽）分别为 3.92 mm 和 3.76 mm，接近圆形高斯光束。此时泵浦光束的直径约为 4 mm。

利用压电光学调整架精准控制腔镜的偏角，实现对 OPO 腔失谐特性的定量研究。对每个腔镜在其理想准直位置附近各进行两个方向的角度扫描，得到输出能量随失谐角度 δ_x 的变化如图 3 中的二维图所示（所有能量值均采用 Newport 919E-0.1-12-25K 能量计测得）。理想准直位置对应的失谐角度 $\delta_x=0$，下标 $x=1\sim4$ 分别对应压电促动器的轴 1～4。图 3 中的 4 条曲线为沿各主轴方向的包络（其他三个方向的偏角 $\delta=0$）。在泵浦光束直径为 4 mm、腔长 L 为 65 mm、输出脉冲能量为 6.6 mJ 的条件下，测得 4 个方向的半峰全宽（称为“对准容限”）分别为 0.171、1.861、0.177、1.933 mrad。腔镜倾斜引起了信号光的几何偏折损耗，经过有限次往复后信号光偏折出由泵浦光束形成的增益区，导致 OPO 输出下降。从图 3 中可以看出前后两个腔镜的同一轴向（轴 1 与轴 3、轴 2 与轴 4）的差异不明显。交换前后镜架得到了相近的结果。水平方向（轴 2 和轴 4，对应晶体的 y 介电主轴）的对准容限约为垂直方向（轴 1 和轴 3，对应晶体的 x-z 介电主平面）的 10 倍。将晶体和泵浦光偏振态同步旋转 90°也得到了相近的结果，排除了不同促动器间硬件差异的影响。

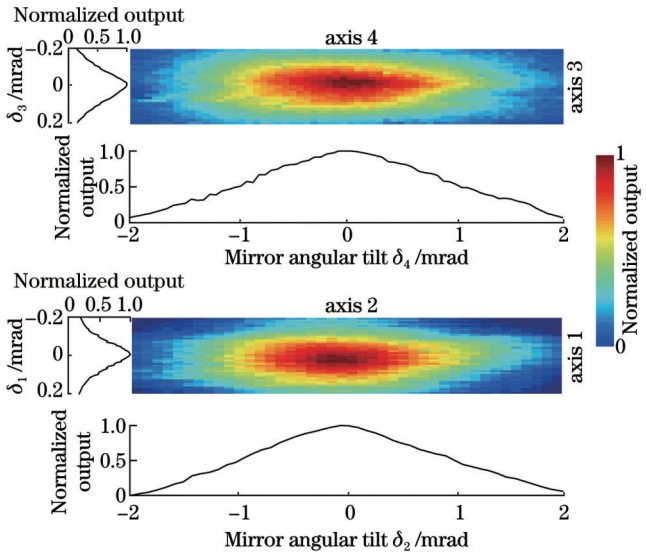

图 3　OPO 输出能量随腔镜不同方向失谐角度的变化

Fig. 3　OPO output versus cavity mirror misalignment angle in different directions

上述不同方向上对准容限的显著差异是由该 OPO 的临界相位匹配形式导致的。KTP 晶体的 3 个介电主轴和通光方向如图 4 所示，极角 $\theta=60°$、方位角 $\varphi=0°$。泵浦光（p）和闲频光（i）沿 y 主轴偏振，为寻常

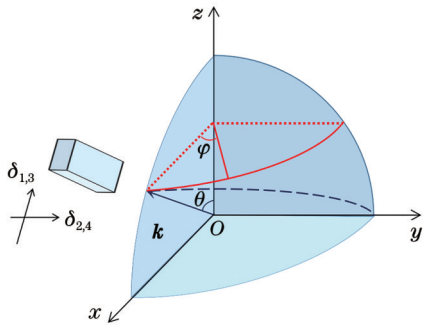

图 4　KTP 晶体介电主轴及晶向示意图

Fig. 4　Schematic of KTP principal dielectric axes and crystallographic orientation

光，折射率分别为 $n_p=n_{py}$ 和 $n_i=n_{iy}$，与 θ 和 φ 都无关。信号光(s)在 x-z 主平面内偏振，为非寻常光，其折射率与 θ 有关而与 φ 无关，表达式为

$$n_s(\theta)=\frac{n_{sx}n_{sz}}{\sqrt{n_{sz}^2\cos^2\theta+n_{sx}^2\sin^2\theta}},\tag{1}$$

式中：n_{sx}、n_{sy}、n_{sz} 分别为信号光(s)在 x、y、z 方向上的主轴折射率。

根据图 4 所示的几何关系，在 $\theta=60^\circ$ 和 $\varphi=0^\circ$ 处，腔镜失谐角 $\delta_{1,3}$ 引起光束 θ 角度偏折，失谐角 $\delta_{2,4}$ 引起光束 φ 角度偏折(在虚线大圆与小圆切点附近的小范围内成立)。波矢失配量 Δk 对不同方向失谐角的敏感程度可写成

$$\left|\frac{\partial(\Delta k)}{\partial\delta_{1,3}}\right|\propto\left|\frac{\partial(\Delta k)}{\partial\theta}\right|=2\pi\left|\frac{1}{\lambda_p}\frac{\partial n_p}{\partial\theta}-\frac{1}{\lambda_i}\frac{\partial n_i}{\partial\theta}-\frac{1}{\lambda_s}\frac{\partial n_s}{\partial\theta}\right|\Bigg|_{\theta=60^\circ},\tag{2}$$

$$\left|\frac{\partial(\Delta k)}{\partial\delta_{2,4}}\right|\propto\left|\frac{\partial(\Delta k)}{\partial\varphi}\right|=2\pi\left|\frac{1}{\lambda_p}\frac{\partial n_p}{\partial\varphi}-\frac{1}{\lambda_i}\frac{\partial n_i}{\partial\varphi}-\frac{1}{\lambda_s}\frac{\partial n_s}{\partial\varphi}\right|\Bigg|_{\varphi=0^\circ}。\tag{3}$$

在方位角 $\varphi=0^\circ$ 处，泵浦光、闲频光、信号光的折射率都与 φ 无关，因此式(3)右侧为 0。当 $\theta=60^\circ$ 时，信号光的折射率与 θ 有关，由式(1)可得

$$\frac{\partial n_s}{\partial\theta}=\frac{n_{sx}n_{sz}(n_{sz}^2-n_{sx}^2)\sin\theta\cos\theta}{(n_{sz}^2\cos^2\theta+n_{sx}^2\sin^2\theta)^{3/2}}。\tag{4}$$

根据 KTP 晶体的色散属性，将信号光(波长 820 nm)的主轴折射率代入式(4)和式(2)，求出 $\theta=60^\circ$ 时 $|\partial(\Delta k)/\partial\theta|=6.61\times10^5\ \mathrm{m^{-1}\cdot rad^{-1}}$。因此，$|\partial(\Delta k)/\partial\delta_{1,3}|\gg|\partial(\Delta k)/\partial\delta_{2,4}|$。轴 1 和轴 3 方向的对准容限更小，输出能量对此方向的失谐更为敏感。

利用不同大小的光阑改变泵浦光束的尺寸，重复图 3 所示的测量。在给定泵浦光强度 28.6 MW/cm^2 和腔长 65 mm 的情况下，各方向的对准容限随光束尺寸的增加而增大[如图 5(a)所示]，因为较大的互作用区域(重叠区)可以对偏离轴向的信号光提供更多的有效往复增益次数。在固定光束直径为 4 mm 和腔长为 65 mm 的条件下，调整可变衰减器改变泵浦光强，得到对准容限随输出能量的变化曲线，如图 5(b)所示。各方向的对准容限随输出能量的增加而增大，因为更高的泵浦光强能够提供更高的单程增益[21]，更容易建立振荡。

改变 OPO 腔长，观察输入能量不变和输出能量不变两种情况下对准容限的变化，结果如图 6 所示。在输入能量一定的条件下，对准容限随腔长的增加而减小，如图 6(a)所示。这是因为离轴光束可以在较短的腔中有效往复更多次(记为因素 1)。随着腔长从 40 mm 增加到 65 mm 再增加到 90 mm，33 mJ 绿光泵浦分别产生了 6.5、5.2、3.6 mJ 的闲频光输出。为保持输出

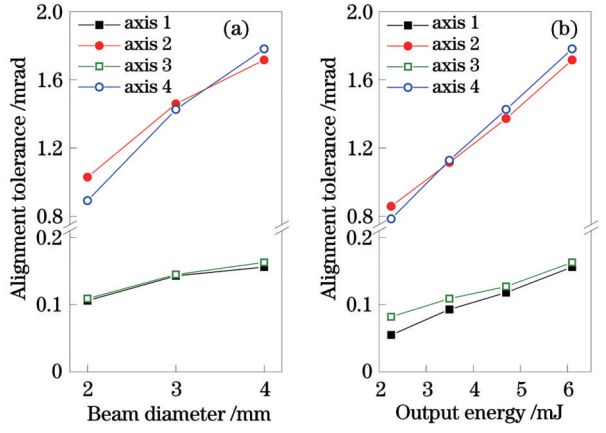

图 5　对准容限与泵浦光束直径和输出能量的关系。(a)对准容限与光束直径的关系；(b)对准容限与输出能量的关系

Fig. 5　Dependence of alignment tolerance on pump beam diameter and output energy. (a) Dependence of alignment tolerance on pump beam diameter; (b) dependence of alignment tolerance on output energy

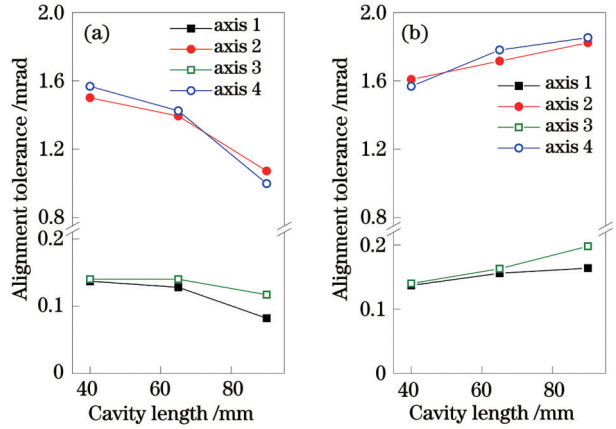

图 6　在输入和输出能量不变的情况下对准容限与腔长的关系。(a)在输入能量不变的情况下；(b)在输出能量不变的条件下

Fig. 6　Alignment tolerance as functions of cavity length at given input and output energies. (a) At given input energy; (b) at given output energy

水平(6.2 mJ)不变,当腔长增加时,须适当将输入泵浦光能量从32 mJ提高到36.6 mJ再提高到42 mJ。此时,可以观察到对准容限略有增大,如图6(b)所示。由于较长腔OPO使用的泵浦光强度更高,因而单程增益更高(记为因素2)。上述两个因素叠加共同导致了图6(b)中对准容限的略微增大。

腔长的改变也会引起OPO其他输出特性的变化。腔长增大导致OPO起振阈值升高(10.7 mJ→13.3 mJ→18.3 mJ)、斜率效率降低(28.7%→26.2%→25.3%),这可用此前的理论模型解释[19]。利用热释电相机测量输出光束的模场分布和发散角,结果显示,三种腔长下的OPO均产生了接近圆形的高斯光束,水平和垂直方向的发散角近似相等。由图7可以看出,随着腔长从40 mm增加到65 mm再增加到90 mm,若要保持输出能量为6.1 mJ,则相应的输入泵浦光能量分别为31.5、36.5、41.5 mJ(光束直径为4 mm)。由图8可以看出,输出光束的发散角随着腔长的增加而减小。对于长度为90 mm的OPO腔,在输出能量为6.1 mJ时,水平和垂直方向上的腰斑直径分别为3.09 mm和3.16 mm,估算两个方向的光束质量因子分别为8.26和8.87。可以看出,增加腔长能够改善光束质量,但脉冲能量的稳定性会变差,脉冲能量波动的方均根值增大(3.09%→3.61%→3.96%)。

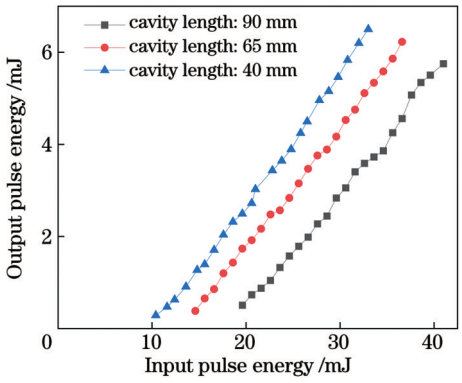

图7 不同腔长下KTP-OPO的输入-输出关系

Fig. 7 Input-output relationship of KTP-OPO with different cavity lengths

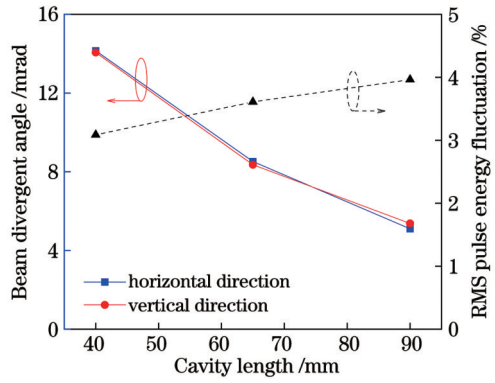

图8 输出光束水平和垂直方向发散角以及脉冲能量波动的方均根随腔长的变化

Fig. 8 Variation of output beam divergent angles in horizontal and vertical directions and root-mean-square (RMS) pulse energy fluctuation with cavity length

4 结 论

本文研究了平行平面腔OPO的腔镜失谐特性。基于这种腔型结构的OPO作为宽调谐相干光源已被广泛采用。利用532 nm绿光脉冲泵浦的KTP晶体,通过临界相位匹配产生1514 nm波长,获得了近圆形高斯光斑,斜率效率不低于25%,脉冲能量波动的方均根值不大于4%。利用压电光学调整架精准控制腔镜的偏角,实现了对OPO腔失谐特性的定量研究。实验中观察到该OPO输出对临界方向(极角)失谐的敏感程度远高于对非临界方向(方位角)失谐的敏感程度,通过分析相位失配解释了这一现象。扩宽泵浦光束和提高泵浦光强可以增大谐振腔的对准容限。在输入和输出脉冲能量一定的条件下,分析了腔长对腔镜对准容限及其他输出特性的影响。上述结论适用于脉冲运转、平行平面腔、临界相位匹配的OPO。

参 考 文 献

[1] Sutherland R L. Handbook of nonlinear optics[M]. 2nd ed. New York: Marcel Dekker Inc, 2003: 121-240.

[2] Ding Y J. Progress in terahertz sources based on difference-frequency generation[J]. Journal of the Optical Society of America B, 2014, 31(11): 2696-2711.

[3] 刘鹏翔, 李伟, 郭丽媛, 等. 基于有机吡啶盐晶体的太赫兹频率上转换探测[J]. 物理学报, 2021, 70(5): 050701.
Liu P X, Li W, Guo L Y, et al. Terahertz wave up-conversion detection based on organic nonlinear optical crystals[J]. Acta Physica Sinica, 2021, 70(5): 050701.

[4] Haidar S, Miyamoto K, Ito H. Generation of continuously tunable, 5-12 μm radiation by difference frequency mixing of output waves of a KTP optical parametric oscillator in a $ZnGeP_2$ crystal[J]. Journal of Physics D: Applied Physics, 2004, 37(23): 3347-3349.

[5] 孟君, 丛振华, 赵智刚, 等. 百赫兹大能量KTA双波长光参量振荡器[J]. 中国激光, 2021, 48(12): 1201009.
Meng J, Cong Z H, Zhao Z G, et al. 100 Hz high-energy KTA dual-wavelength optical parametric oscillator[J]. Chinese Journal of Lasers, 2021, 48(12): 1201009.

[6] 魏磊, 李宝, 陈国, 等. 长波红外CdSe光参量振荡器[J]. 中国激光, 2021, 48(24): 2401004.
Wei L, Li B, Chen G, et al. Long-wave infrared CdSe optical parametric oscillator[J]. Chinese Journal of Lasers, 2021, 48(24): 2401004.

[7] Liu P X, Guo L Y, Qi F, et al. Large dynamic range and wideband mid-infrared upconversion detection with $BaGa_4Se_7$ crystal[J]. Optica, 2022, 9(1): 50-55.

[8] 周炳琨, 高以智, 陈倜嵘, 等. 激光原理[M]. 6版. 北京: 国防工业出版社, 2009.
Zhou B K, Gao Y Z, Chen T R. Laser principle[M]. 6th ed. Beijing: National Defense Industry Press, 2009.

[9] Freiberg R J, Halsted A S. Properties of low order transverse modes in argon ion lasers[J]. Applied Optics, 1969, 8(2): 355-362.

[10] Snopko V N, Tsaryuk O V. Polarization and energy characteristics of CO_2 laser radiation with misalignment of the resonator mirrors [J]. Journal of Applied Spectroscopy, 1985, 42(4): 391-394.

[11] Hauck R, Kortz H P, Weber H. Misalignment sensitivity of optical resonators[J]. Applied Optics, 1980, 19(4): 598-601.
[12] Min L H, Vogler K. Misalignment sensitivity of Nd:YAG unstable resonator with self-filtering aperture[J]. Optics Communications, 1990, 76(5/6): 357-362.
[13] Laporta P, Brussard M. Misalignment sensitivity of laser-diode pumped solid-state lasers[J]. Optics Communications, 1991, 85(1): 47-53.
[14] 王绍民. 失调激光系统的矩阵和图论处理方法[J]. 杭州大学学报(自然科学版), 1979, 6(3): 42-52.
Wang S M. Matrix and flow-graph methods in misalignment laser systems[J]. Journal of Hangzhou University (Nature Science), 1979, 6(3): 42-52.
[15] 方洪烈, 王小异. 失调平面腔的解析线: 多尺度微扰论在谐振腔理论中的应用[J]. 光学学报, 1984, 4(12): 1107-1110.
Fang H L, Wang X Y. Analytic solutions to the misaligned flat mirror resonators-applications of the multiple-scaling perturbation theory to optics resonators[J]. Acta Optica Sinica, 1984, 4(12): 1107-1110.
[16] 吕百达. 光学谐振腔的失调特性[J]. 量子电子学, 1986, 3(1): 91-97.
Lü B D. Misalignment characteristics of optical resonators[J]. Chinese Journal of Quantum Electronics, 1986, 3(1): 91-97.
[17] 胡亚红, 邓年茂, 何俊华, 等. 激光谐振腔自动稳定调节的一种方法[J]. 光子学报, 2001, 30(7): 871-874.
Hu Y H, Deng N M, He J H, et al. A mean on laser resonator auto-stability adjustion[J]. Acta Photonica Sinica, 2001, 30(7): 871-874.
[18] 姚宝权, 王月珠, 柳强, 等. KTP光学参量振荡器输出激光的空间模式和光束质量[J]. 中国激光, 2001, 28(8): 693-697.
Yao B Q, Wang Y Z, Liu Q, et al. Study of the spatial beam quality of KTP optical parametric oscillator[J]. Chinese Journal of Lasers, 2001, 28(8): 693-697.
[19] Harris S E. Tunable optical parametric oscillators[J]. Proceedings of the IEEE, 1969, 57(12): 2096-2113.
[20] Kreuzer L B. Single mode oscillation of a pulsed singly resonant optical parametric oscillator[J]. Applied Physics Letters, 1969, 15(8): 263-265.
[21] Brosnan S J, Byer R L. Optical parametric oscillator threshold and linewidth studies[J]. IEEE Journal of Quantum Electronics, 1979, 15(6): 415-431.

Characteristics of Mirror Misalignment of Plane-Parallel Cavity-Based Optical Parametric Oscillators

Fu Qiaoqiao[1,2,5], Liu Pengxiang[1,2,4*], Qi Feng[1,2,4], Li Weifan[1,2,4], Niu Chuncao[1,2,3], Li Wei[1,2,3], Guo Liyuan[1,2], Wang Yelong[1,2,4], Liu Zhaoyang[1,2,4]

[1]*Shenyang Institute of Automation, Chinese Academy of Sciences, Shenyang* 110169, *Liaoning, China*;
[2]*Key Laboratory of Liaoning Province in Terahertz Imaging and Sensing, Shenyang* 110169, *Liaoning, China*;
[3]*College of Information Engineering, Shenyang University of Chemical Technology, Shenyang* 110142, *Liaoning, China*;
[4]*Institutes for Robotics and Intelligent Manufacturing, Chinese Academy of Sciences, Shenyang* 110169, *Liaoning, China*;
[5]*University of Chinese Academy of Sciences, Beijing* 100049, *China*

Abstract

Objective Optical parametric oscillators (OPOs) have been proven to be effective, coherent light sources that can expand the wavelengths of commercial lasers (typically limited to narrow emission lines and bands) to a broad range from visible to far-infrared bands. *Q*-switched lasers with high peak powers have significantly promoted the development and applications of OPOs with the following advantageous characteristics: system compactness (for example, two cavity mirrors and a nonlinear crystal), relatively high conversion efficiency, singly resonant operation, and frequency-agile tunability (for example, angle tuning). A plane-parallel cavity with a large mode volume is well-suited for *Q*-switched laser pumps. This type of OPO is widely adopted, for example, as a pump/seed source in nonlinear terahertz or mid-infrared (MIR) generation or directly as an MIR source, owing to the wide tuning range and ease of construction. As the earliest configuration in a laser resonator, a plane-parallel cavity is critically stable and sensitive to mirror misalignment. The misalignment of laser cavities, including those of argon ion, CO_2, and Nd:YAG lasers, has been analyzed previously; however, studies on OPO cavities have rarely been reported. In this study, we performed an experimental investigation on the misalignment characteristics of a plane-parallel cavity-based OPO.

Methods In this study, an OPO based on a plane-parallel cavity structure was developed. A potassium titanyl phosphate (KTP) crystal was utilized as the nonlinear medium (cut at $\theta=60^\circ$, $\varphi=0^\circ$, and 10 mm×7 mm×20 mm, anti-reflection (AR)-coated at 532 nm/800–900 nm/1300–1600 nm). A frequency-doubled Nd∶YAG laser (532 nm, 10 ns, and 10 Hz) was employed as the pump source. Two flat mirrors (AR-coated at 532 nm/1300−1600 nm and highly reflection-coated at 800–900 nm) formed a singly resonant cavity. The ns-pulsed OPO was operated at a wavelength of 1514 nm via o → e (signal) + o (idler) critical phase matching. The cavity mirrors were precisely controlled using piezoelectric optical mounts for alignment. Each mount was equipped with two piezo actuators, which could provide a two-dimensional (2D) adjustment (axes 1 and 2 for output mirror M1 and axes 3 and 4 for input mirror M2) with an angular resolution of $\leqslant 0.7$ μrad.

Results and Discussions Typical output results (pulse envelopes and beam profile) of the KTP-OPO are presented in

Fig. 2. The piezoelectric optical mounts with a motion controller module facilitate quantitative analysis of the influence of mirror misalignment on the OPO output. The variation in the output pulse energy with angular tilt δ_x is measured while scanning each cavity mirror along two directions around the well-aligned position ($\delta_x=0$), as presented by the 2D graphs in Fig. 3. The subscripts $x=1-4$ correspond to the four actuators, axes 1 - 4, respectively. The four curves presented in Fig. 3 present envelopes along the principal axis (with the other three $\delta=0$). The full widths at half maximum of the curves (called "alignment tolerance") from axes 1 to 4 are 0.171, 1.861, 0.177, and 1.933 mrad, respectively, which are determined at a pump beam diameter $\Phi=4$ mm, cavity length $L=65$ mm, and output pulse energy=6.6 mJ. The discrepancy between the two mirrors along the same direction (axes 1 and 3 and axes 2 and 4) is minimal, which is verified by alternating the two mounts. The tolerances along the horizontal direction (axes 2 and 4, y-principal dielectric axis) are approximately 10 times those along the vertical direction (axes 1 and 3, x-z-principal plane). This can be attributed to the critical phase matching configuration (Fig. 4). As presented in Fig. 5(a), the alignment tolerance increases with the beam size at a specific pump intensity and cavity length because a larger interaction region (cross-section) can provide more effective round trips for misaligned signal beams. The relationship between the tolerance and output energy, shown in Fig. 5(b), demonstrates an increasing trend because a higher output energy corresponds to a higher single-pass gain (easier to build up). The alignment tolerances of different cavity lengths are compared at fixed input [Fig. 6(a)] and output pulse energies [Fig. 6(b)]. In addition, the other output characteristics vary with the OPO cavity length. A longer cavity length results in a higher threshold and lower energy conversion efficiency (Fig. 7). The divergent angles decrease with the cavity length at approximately equal output energies and beam sizes (left y-axis of Fig. 8). Better beam quality and worse stability can be obtained with a more extended cavity (right y-axis of Fig. 8), and the root-mean-square (RMS) of pulse energy fluctuation increases (3.09%→3.61%→3.96%).

Conclusions Herein, we quantitatively characterize the mirror misalignment of a plane-parallel cavity-based OPO, which has been widely utilized as a convenient coherent light source with a desired wavelength. A green laser-pumped KTP-OPO equipped with piezoelectric optical mounts is constructed. An almost circular Gaussian beam with a wavelength of 1514 nm is delivered with a slope efficiency of $\geqslant$25% and a pulse energy fluctuation (RMS) of $\leqslant$4%. The output shrinkage is measured by scanning the cavity mirrors around a well-aligned position. The alignment appears to be significantly more sensitive in the critical direction than in the noncritical direction, which can be explained based on the phase-matching configuration. The alignment tolerance increases with the beam size and input intensity. In addition, the cavity length dependence is analyzed at specific input and output pulse energies. This paper presents a type of ns-pulsed, singly resonant, and critical phase-matched OPO with a wide-angle tuning capability.

Key words nonlinear optics; optical parametric oscillator; plane-parallel cavity; misalignment tolerance; critical phase matching